Lab on a Chip

Devices and applications at the micro- and nanoscale

Accepted Manuscript

This article can be cited before page numbers have been issued, to do this please use: M. E. Blaha, S. Hasan, C. Dusny and D. Belder, *Lab Chip*, 2022, DOI: 10.1039/D2LC00032F.

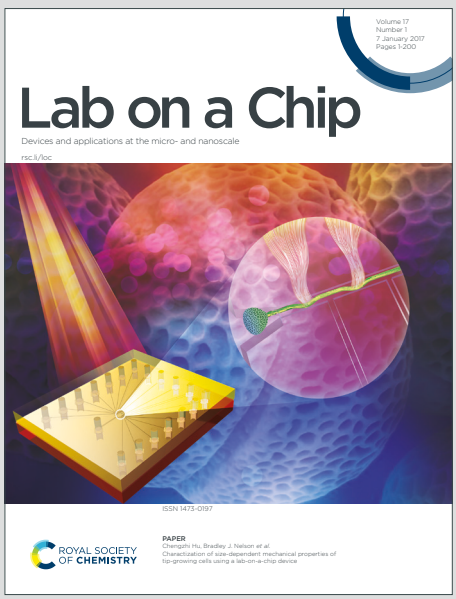

ROYAL SOCIETY OF CHEMISTRY

rsc.li/loc

View Article Online
DOI: 10.1039/D2LC00032F

ARTICLE

Fluorescence lifetime activated droplet sorting (FLADS) for label-free sorting of *Synechocystis* sp. PCC6803

fiReceived 00th January 20xx,
Accepted 00th January 20xx

DOI: 10.1039/x0xx00000x

Maximilian Emanuel Blaha[a], Sadat Hasan[a], Christian Dusny[b], and Detlev Belder*[a]

This study presents the label-free sorting of cyanobacterial cells in droplets with single-cell sensitivity based on their fluorescence lifetime. We separated living and dead cyanobacteria (*Synechocystis* sp. PCC6803) using fluorescence lifetime signals of the photopigment autofluorescence to indicate their photosynthetic activity. We developed a setup and a chip design to achieve live/dead sorting accuracies of more than 97 % at a droplet frequency of 100 Hz with a PDMS-based chip system and standard optics using fluorescence lifetime as the sorting criterion. The obtained sorting accuracies could be experimentally confirmed by cell plating and observing the droplet sorting process via a high-speed camera. The herein presented results demonstrate the capabilities of the developed system for studying the effects of stressors on cyanobacterial physiology and the subsequent deterministic sorting of different stress-response phenotypes. This technology eliminates the need for tedious staining of cyanobacterial cells, which makes it particularly attractive for its application in the field of phototrophic microbial bio(techno)logic and in the context of cell secretion studies.

Introduction

Droplet-based microfluidics is a subcategory of microfluidics and allows the manipulation of discrete volumes of micro- to femtoliters of fluids in immiscible phases.[1–3] This allows the parallelization, compartmentalization, and miniaturization of experiments[1,2], which is a practical and established feature in chemical synthesis [4,5] and high-throughput drug screening. [6,7] When coming to potential biological and biomedical applications, droplet microfluidics offers the feature of single-cell incubation, analysis [8–11], and sorting. [12,13]

A crucial aspect of cell analysis and sorting is the detection technique used. Fluorescence is the most widely used technique in microfluidics and droplet microfluidics [14] and is valued for its simplicity and effectiveness.[15] The fluorescence-based analysis of cells in droplets usually involves including fluorescent dyes in the process [16,17], complicating the workflow and potentially altering the samples.[18]

A potential label-free cell detection technique would overcome these limitations. In the past decades, label-free approaches as optical absorbance[19], Raman scattering [20], mass spectrometry [21], and image recognition [13,22,23] have been investigated. However, these techniques have their own set of advantages and disadvantages. *E.g.*, Mass spectrometry gives structural information but is destructive and slow. Raman scattering gives structural information, is non-destructive, but the low optical gain limits the throughput. Therefore, novel tools that can provide another criterion to distinguish cells will be of great use to expand the scope of droplet sorting for cell differentiation in various applications.

When excited at appropriate wavelengths, label-free cell detection can also be achieved by intrinsic fluorescence of proteins or other intrinsic fluorophores such as NAD(P)H [24,25] or chlorophylls [25,26]. However, staining-free analysis of cells is limited to the given fluorophores, which leads to the problem that cells can hardly be distinguished based on the fluorescence intensity of these fluorophores alone. Fluorescence lifetime is a viable option for solving this problem since it complements intensity-only measurements. In comparison to bare intensity measurements, which depend on the concentration of the fluorophore, the duration of light exposure, and the excitation wavelength, fluorescence lifetime is affected particularly by the chemical structure of the molecule, temperature, solvent environment, and the presence of fluorescence quenchers.[25]

While some studies have described fluorescence lifetime-activated cell sorting (FLACS) [27–29], corresponding label-free studies in microfluidics are extremely scarce.[30]

In particular, the field of label-free fluorescence lifetime activated cell sorting in microfluidic droplets is largely unexplored. This is especially true for the field of high-throughput sorting, which is limited by the ability to determine fluorescence lifetimes at high rates. In our previous works [31,32] we developed an approach for label-free fluorescence lifetime activated droplet sorting and showed its potential to distinguish model substances. In this study, we also demonstrated the suitability of the approach for cell sorting of yeast cells using two-photon excitation, but we were not yet able to reach the single-cell level and were limited to low sorting frequencies of 1 - 2 Hz.[31,32]

[a] *Institute for Analytical Chemistry, Leipzig University, Linnéstraße 3, 04103 Leipzig, Germany.*
[b] *Department Solar Materials, Helmoltz-Centre for Environmental Research – UFZ Leipzig, Permoserstr. 15, 04318 Leipzig, Germany.*
Electronic Supplementary Information (ESI) available. See DOI: 10.1039/x0xx00000x

View Article Online DOI: 10.1039/D2LC00525

This is now targeted in the current study to distinguish and sort living and dead cyanobacterial cells. We choose *Synechocystis* sp. PCC6803 as a model system due to its ubiquitous occurrence and importance for ecosystems and modern photobiotechnology.[33–38] The fluorescence lifetime properties of cyanobacteria are also the subject of current research.[26,39–42] These aspects make cyanobacteria an optimal candidate for establishing the technology of label-free fluorescence lifetime activated cell sorting in droplets for research on phototrophic microorganisms and later studying their secretion and heterogenity.[43]

This study describes the development of a system capable of sorting live and dead cyanobacteria based on their autofluorescence lifetime in droplets in high-throughput. We start with analyzing the basic fluorescence and fluorescence lifetime properties of cyanobacteria using fluorescence lifetime imaging microscopy (FLIM). Furthermore, we describe the process and development of bringing the static analysis to in-flow mode and adding a sorting feature with high accuracy. Integrating a high-speed camera and adopted lenses made it possible to achieve high sorting accuracy at high throughput.[44] The accuracy of the developed method was confirmed by culturing sorted life and dead cell fractions on agar-agar plates. In a further step, we analyzed the influence of various factors like toxins, environmental factors, and sub-strain-specific physiology on the fluorescence lifetime of the photosynthetic machinery, getting insight into the heterogeneity of physiological response to external stressors with single-cell resolution.

Materials and Methods

Optical Setup

The optical setup used is similar to our previous study[31]. A time-resolved Confocal Microscope platform (MT200, PicoQuant, Germany) with an IC71 microscope (Olympus, Germany) was used to detect fluorescence lifetimes. A 405 nm picosecond pulsed diode laser (LDH-D-C-405, PicoQuant, Germany) at a repetition rate of 80 MHz driven by a PDL-828-S pulsed laser diode driver (PicoQuant, Germany) was used as a light source. After passing a clean-up filter, the light was fed into a single-mode fiber. For the detection, a 10× UPlanFl objective (Olympus, Germany) was used. The fluorescence emission was collected through the same lens, passed a long-pass filter (510 nm for sorting and its preliminary experiments and 420 nm for testing the influence of stressors), a dichroic mirror (420 dcxr, chroma, USA), a tube lens, and a 150 µm pinhole. For detection, a single-photon avalanche diode (SPAD) was used (PDM series, Micro Photon Devices, Italy). The laser's synchronization signal and the SPAD output were collected by a time-correlated single-photon counting (TCSPC) unit (PicoHarp 300, PicoQuant, Germany). A LabVIEW (LabVIEW 2017, National Instruments, USA) program processed the collected data from the TCSPC. The optical setup is shown in Figure 5.

Chip design, fabrication, and assembly

The PDMS (Dow Corning, MI, USA) chips were produced using standard soft lithography described in our previous study[30]. The soda-lime-glass bottom (76×26×1 mm, Thermo Scientific, USA) of the chip was spin-coated (4000 rpm for 60 s) with a thin PDMS-layer (20 µm). The Top layer containing the channel structures and the PDMS coated bottom were bonded using oxygen plasma. The electrode channels were filled with an alloy with a melting point of 58°C (Sonderweichlot 302, S-Bi49In21Pb18Sn12, Chemet GmbH, Germany) using a hot plate. The used chip design is displayed in Figure 4.

LabVIEW-Programming

TCSPC output is processed by our previously developed program EasyFlux, available as open-source software (https://github.com/SadatHasan/EasyFlux). The software allows fluorescence intensity and fluorescence lifetime analysis in real-time. Several features were added to make the software capable of cell sorting. The number of photons considered for every calculated average fluorescence lifetime is now recorded, and the computed fluorescence lifetimes are now plotted in a histogram. Furthermore, a feature was added which allows deciding if fluorescence lifetimes above or below the chosen threshold are initiating a TTL-pulse with the help of a date acquisition (DAQ) device (USB 6000, National Instrument, USA).

Electronics

The DAQ-Pulse triggers a dual-channel signal generator (Rigol Technologies, DG 1032 dual-channel, China), which provides 10 volts in 10 kHz as a square wave (50% duty cycle). The signal generator outputs are amplified 200x using a pair of high voltage amplifiers (Trek-2220, Trek Inc., USA) and actuate the sorting channels electrode pairs of the chip.

Fluorescence Lifetime Calculation

Fluorescence lifetimes were calculated by counting single-photon arrival time from the TCSPC. Photons were collected and put into a histogram with a length of 12.5 ns. All calculated fluorescence lifetimes are average fluorescence lifetimes $\overline{\boldsymbol{\tau}}$ and are calculated as given in equation 1. $\boldsymbol{I_i}$ indicates the number of photons in every time step of the TCSPC histogram. $\boldsymbol{t_i}$ indicates the time at every timestep in the histogram.[25]

$$\overline{\boldsymbol{\tau}} = \frac{\sum_i^n \boldsymbol{I_i t_i}}{\sum_i^n \boldsymbol{I_i}} \qquad \mathbf{1}$$

Cell sorting experiments

Novec™ 7500 (3M, Germany) was used as a continuous phase, which contained 0.5 % Pico-surf (Sphere Fluidics Limited, Cambridge, UK) at the droplet generation area. For the spacing of the droplets, pure Novec™ 7500 was used. The cell concentration was optimized until ~ 10-30 % of the droplets contained a cell to ensure single-cell encapsulation.[44] For the droplet generation, pressure-based pumps (Fluigent, FlowEZ, Germany) were used. The pressures were adjusted until a droplet frequency of 60 - 100 Hz was reached. For detection,

View Article Online
DOI: 10.1039/D1LC00032F

the described optical setup was used with a laser power of 220 µW. For observing the sorting, the upper beam path was equipped with a 470 nm LED (470L3, Thorlabs, Germany) and a 470/40 bandpass filter. A high-speed camera (Phantom VEO 410L high speed, Phantom Ametek, Germany) was used with a 20× LUCPlan-FL Objective (Olympus, Germany). 100 µl of buffer were pipetted inside the outlets to prevent drying out. After every hour, the buffer in the outlets was collected and replaced by fresh buffer. Droplets were demulsified using 100 µL of 1H,1H,2H,2H-Perfluoro-1-octanol (PFO) (fluorochem, United Kingdom).

Cyanobacteria preparation and accuracy analysis

Synechocystis sp. PCC6803 was grown photoautotrophically in yBG11 medium buffered with 10 mM HEPES at pH 7.2.[45] The cell cultures were incubated in growth chambers (Minitron LED Option HT) at 30°C under continuous illumination with 50 µmol photons m^{-2} s^{-1}. If not stated differently, cells were grown in baffled Erlenmeyer flasks at 10% filling volume under continuous shaking at 150 rpm with an amplitude of 2.5 cm under ambient CO_2 (air). The chamber humidity was kept constant at 75% relative saturation. To prepare dead cells, 1 ml of the cell suspension was harvested and centrifuged at 14000 g for 10 min and resuspended in yBG11 medium containing 4 % formaldehyde, freshly prepared from solid paraformaldehyde (PFA) stock. The cell suspension was stored overnight to yield a non-viable (dead) culture of *Synechocystis* sp. PCC6803. The fixed cells were centrifuged and resuspended in fresh buffer three times to remove any traces of PFA. The dead fraction was mixed with fresh cells to give a 1:1 mix of dead and live cells. This mix was diluted until single-cell encapsulation in droplets was statistically achieved. Next to the *Synechocystis* sp. PCC6803 wild-type strain, an *ndhB*-deficient mutant (M55) of *Synechocystis* sp. PCC6803 was prepared and analyzed in the same way as the wild-type strain.[46] For the experimental analysis of the FLADS sorting accuracy, the sorted live and dead fractions were appropriately diluted and plated on solidified yBG11 medium buffered with 10 mM HEPES at pH 7.2,[45] containing 0,75% Agar Agar. The plates were incubated at 50 µmol photons m^{-2} s^{-1} and 30°C until all colonies developed (5-7 days). After incubation, the colonies were counted to determine the sorting accuracy. Untreated cell suspensions were plated as control and reference. Photo-stressed *Synechocystis* sp. PCC6803 cells were obtained by exposing the cell suspension to increased photon flux densities of 200 µmol photons m^{-2} s^{-1} for at least 12 h. Antibiotic stress was induced by culturing the cells yBG11 medium at a Kanamycin concentration 50 µg mL^{-1} (Km 50).

FLIM, UV/VIS, and Fluorimetry

UV/VIS Spectra of the cyanobacteria were recorded using a UV/VIS Spectrometer V-650 (JASCO Research Ltd., Canada) and a cell concentration of 2 × 10^4 cells/µL. A Model FP-6200 fluorimeter (JASCO Research Ltd., Canada) was used for fluorescence spectra with a cell concentration of 1 × 10^4 cells/µL. The upper described optical setup for FLIM-Scans was equipped with a 100× lense (UPlanSApo, Olympus, Germany) with a laser power of 67 µW and a dwell time of 4.0 ms.

Results and DIscussion

This work aimed to develop a system capable of sorting cells inside droplets according to native autofluorescence lifetime properties. Such technology is currently missing for label-free sorting of cells before or after single-cell secretion studies, e.g. in the context of whole-cell biocatalysis. As a model organism, we choose *Synechocystis* sp. PCC6803. They play an important role in our ecosystems regarding their role as ubiquitous occurring photosynthetic active organisms.[33–36] *Synechocystis* sp. PCC6803, and cyanobacteria in general, contain photopigments [47] as a native fluorophore whose fluorescence lifetime can be used to investigate their photosynthetic activity.[48]

One objective of this study was to investigate whether the detection and sorting of photosynthetically active and inactive cyanobacteria in droplets can be achieved at the single-cell level and high throughput using fluorescence lifetime signatures. The system to be developed will then be evaluated for its suitability for screening mutant strains and the differential effects of stressors on Synechocystis sp. PCC6803 at single-cell resolution.

To this end, preliminary investigations had to be carried out to establish a suitable system's technical and scientific basis. 1) Fluorescence and fluorescence lifetime properties of *Synechocystis* sp. PCC6803 needed to be studied and characterized in a physiological steady-state state. 2) The chip and optical systems had to be developed and optimized to allow reliable detection and determination of fluorescence lifetime of Synechocystis sp. PCC6803 at the single cell level in high throughput. 3) After characterizing the spectral properties of the samples and the basic system configuration, the sorting function was realized and evaluated with respect to the achievable sorting accuracy and speed.

UV/VIS, Fluorimetry and FLIM of Cyanobacteria

An important parameter in the development of a fluorescence method on cells with minimal photostress is the UV-VIS spectrum to find the optimal wavelength and minimum exposure intensity. In Figure 1A, the UV/VIS spectrum of living *Synechocystis* sp. PCC6803 (green) is displayed vs. *Synechocystis* sp. PCC6803 stored in buffer containing 4% PFA overnight for fixation referred to as dead (red). The Spectrum shows absorption maxima at 440 nm, 491 nm, 626 nm, and 682 nm, mainly based on chlorophyll- and carotenoid pigments bound in the photosystems of cyanobacteria. The spectra of the two samples do not differ in the location of the absorption maxima or in their intensity. In a further step, we investigated the autofluorescence properties of dye pigments such as chlorophyll a, phycocyanin and phycoerythrin bound in the photosystems of dead and living cyanobacteria in bulk suspensions. 3D Fluorescence spectra of both bulks were recorded after washing *Synechocystis* sp. PCC6803 cell suspensions with fresh buffer. Both 3D spectra of living (Figure

View Article Online
DOI: 10.1039/D2LC00032F

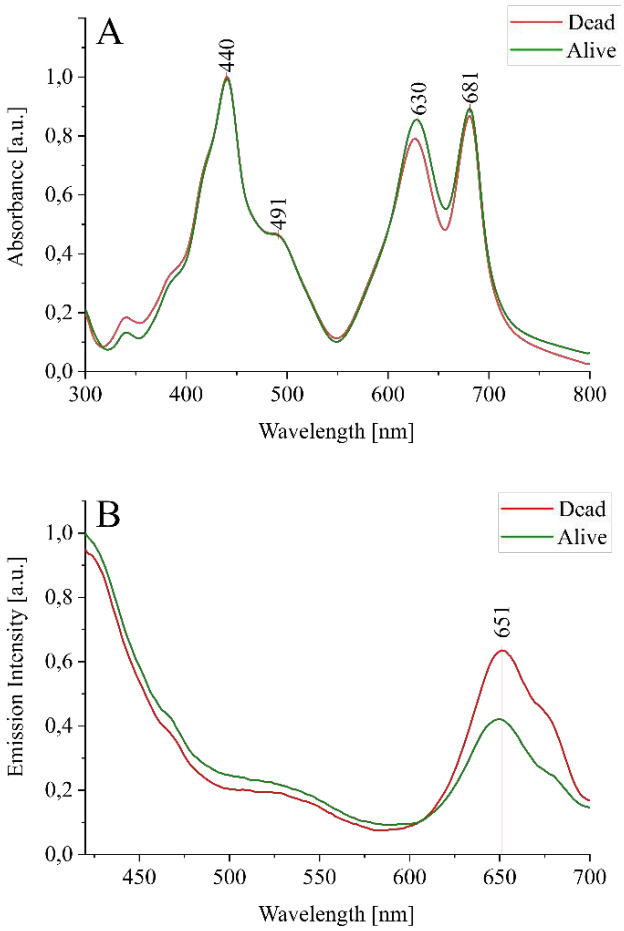

Figure 1: A) UV/VIS Spectra of live and dead cyanobacteria. B) Fluorescence spectra of living and dead cyanobacteria recorded at 405 nm.

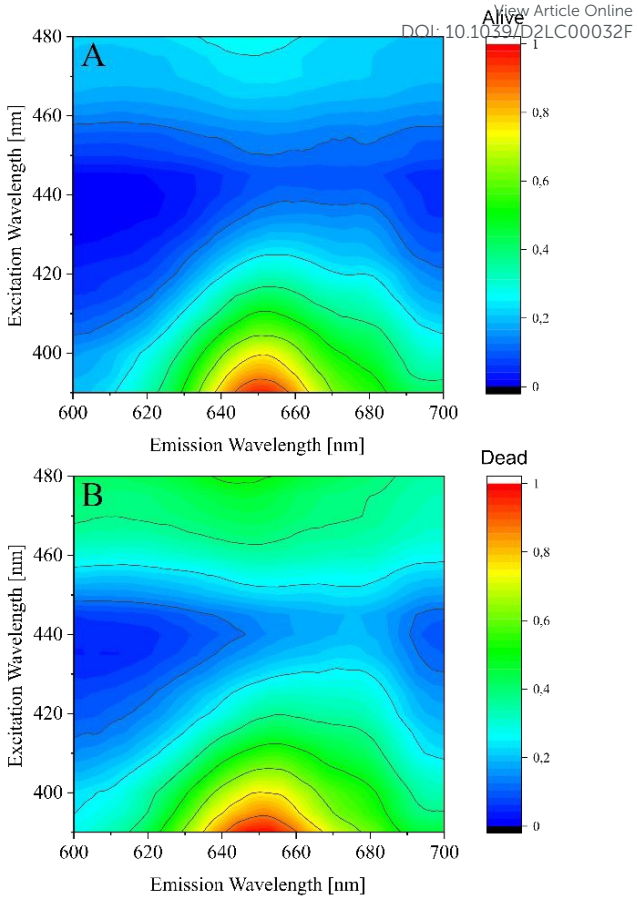

Figure 2: A) 3D Fluorescence spectrum of living cyanobacteria. B)3D Fluorescence spectra of dead cyanobacteria.

2A) and dead (Figure 2B) show a fluorescence maximum at an emission wavelength of 650 nm and excitation wavelength of 390 nm. In comparison, the 3D Fluorescence spectra of dead cells (Figure 2B) show a slightly higher fluorescence intensity than the living cells (Figure 2A). This observation might be attributed to the fully functional state of the photosynthetic machinery in living cells. From a fluorophore standpoint, the energy transition during photosynthesis is a quenching mechanism, resulting in lower fluorescence intensity of photosynthetic active cells.[49,50] However, these differences are not significant enough as a reliable sorting criterium. Based on our spectral characterization of live and dead *Synechocystis* sp. PCC6803, we found 405 nm as an optimal excitation wavelength for all further investigations. With the chosen wavelength, fluorescence spectra for dead and live cells were recorded and are shown in Figure 1B. The spectra show a 30% higher fluorescence intensity for the dead cells at an emission wavelength of 651 nm. As later investigation showed, this promising sorting criterion was only significant in bulk solutions and did not remain on single-cell level.

In further investigation, we used fluorescence lifetime imaging microscopy (FLIM)-scans to investigate the functionality of the photosystems in the cyanobacteria samples. In Figure 3A-C, the recorded FLIM images of live cells (A), dead cells (C) and a mixture of dead and live cells (B) are displayed. Overall, the live cells have a much lower fluorescence lifetime, as indicated by their blue color, while the dead cells have a higher fluorescence lifetime, as indicated by their red color. Dead cells' enhanced fluorescence lifetime is reasoned in the missing quenching, which only appears when photosynthesis occurs, as already discussed. The living cells FLIM-Scan (Figure 3A) also shows a cyanobacterium that died naturally and shows the same characteristics as the fixated cells: an enhanced fluorescence lifetime and a slightly enhanced fluorescence intensity. Using the displayed FLIM-Scans, we extracted how often each lifetime occurred and plotted the data in Figure 3D. This allowed us to clearly quantify the fluorescence lifetime of live cells to ~0.34 ns and the fluorescence lifetime of the dead cells to ~0.64 ns. Furthermore, a clear threshold could be set at a fluorescence lifetime of 0.55 ns which enabled distinguishing living and dead cyanobacteria based on their fluorescence lifetime. This threshold also remained in FLIM-Scans of the mixture of living and dead cells.

Sorting and screening setup

After understanding the optical properties of our samples, we progressed from static bulk measurements to in-flow measurements in droplets at a single-cell concentration. As a

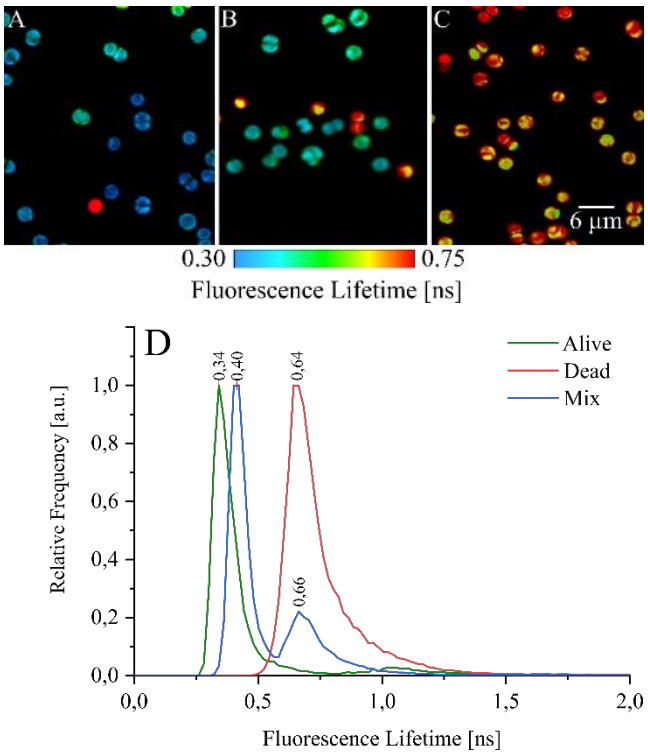

Figure 3: A) FLIM-Scan of living cyanobacteria. Contains one dead cyanobacterium. B) FLIM-Scan of a mixture of live and dead cyanobacteria. C) FLIM-Scan of dead cyanobacteria. D) Histogrammed fluorescence lifetimes from A, B, and C. The fluorescence lifetime at the maximum is marked.

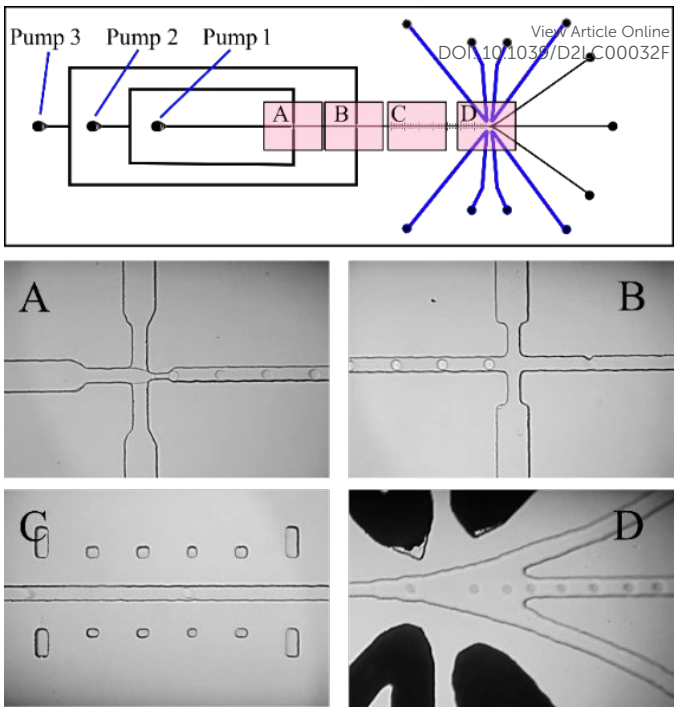

Figure 4: For sorting and screening experiments, used chip design. Blue exaggerated are the electrode pairs used for actuating the droplets. A) Dropletgeneration area. B) Spacing area. C) Detection area with distance markers. D) sorting area with three channels.

basis, we used our already published setup for fluorescence lifetime activated droplet sorting (FLADS)[31] and optimized chip design and optical setup for single-cell sorting and high-throughput measurements.

We used a straightforward chip design, which is displayed in Figure 4. It consists of a flow-focusing droplet generator (Figure 4A) where the cell suspension (dispersed phase) is put in via pump 1, and the continuous phase is put in via pump 2. The dispersed phase was optimized, ending up using 0.5 % Picosurf® in Novec 7500, which allowed a stable and reliable droplet generation and kept the surfactant's concentration as low as possible. The resulting droplets had a diameter of approximately 50 µm and a volume of approximately 40 pL. Furthermore, a spacing area (Figure 4B) was introduced to adjust the droplets' distance to a level desired for later sorting. The spacing area is operated via pump 3 using pure Novec 7500. For detection and actuation of the chip, we used the experimental setup displayed in Figure 5. A 405 nm Laser was used as an excitation source at a repetition rate of 80 Mhz. The excitation light was focused via a microscopic objective in the middle of the channel. The fluorescence was collected via the same lens and guided on a SPAD. The SPAD-Signal is collected via a TCSPC unit and processed using our software EasyFlux, which allows real-time calculations of fluorescence lifetimes.

In a first attempt, we tried if the used setup could detect the cells and determine the fluorescence lifetime of the cells in droplets inflow. The main challenge in our experiments was the low detection probability of the cells, as many cells in the flow were not in laser focus and remained undetected. The detection probability was optimized, reducing the channel dimensions, and trying different microscopic objectives. Regarding the channel dimensions, we found that 55 µm widths × 30 µm height gave us the best compromise of the microfluidic system's high detection probability and reliability. Higher channel dimensions resulted in lower detection probabilities. Lower channel dimensions resulted in an overall instability of the system. Regarding the microscopic objective, we found that 10× lenses with a numerical aperture of n = 0.3 and a working distance of 10 mm gave us the best detection probability. The optimization led to detection probabilities of almost 100% at a droplet frequency of 1 Hz and, based on high-speed camera videos, approximately 20% to 35% at a droplet frequency of 100 Hz. 4× lenses were not capable of detecting any cell. 20× and 40× lenses gave us a drastically reduced detection probability at 1 Hz and a detection probability of virtually zero at higher droplet frequencies between 60 and 100 Hz. Using these optimized parameters, we screened a 1:1 mixture of dead and live cyanobacteria to see if we could differentiate them based on their fluorescence lifetime. In Figure 6A, the intensity feed of the detected cells is displayed. Every peak shows a detected cell in a droplet. Next to it, the calculated average fluorescence lifetime is indicated. In Figure 6B, another intensity feed is shown. Two cell signals are very close to each other in the red encircled area, which shows that our system can detect multiple cells in one droplet and calculate their fluorescence lifetimes independently. After these successful experiments, we determined on-the-fly fluorescence lifetimes of our *Synechocystis* sp. PCC6803 cultures, including live cells, dead cells, and a mixture of both. The fluorescence lifetime

View Article Online
DOI: 10.1039/D2LC00032F

histograms of the cells are displayed in Figure 6C. Our results showed that the fluorescence lifetimes of living cells appear

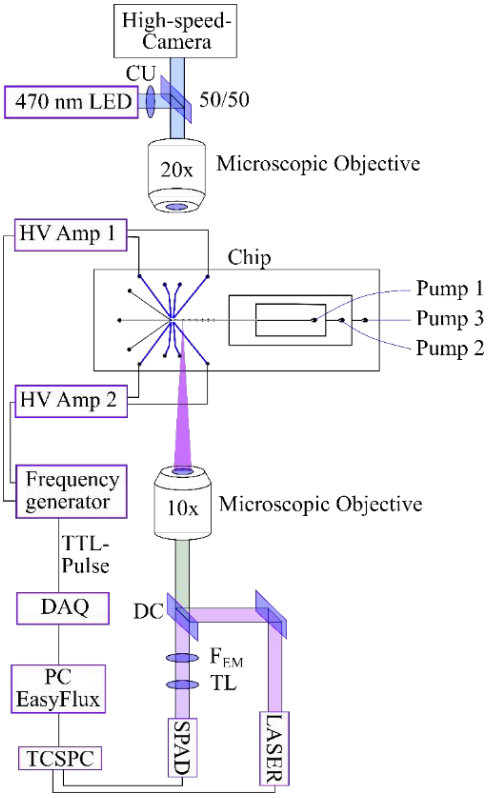

Figure 5: Microfluidic chip as integrated in the optical setup. CU: Cleanup filter, DC: Dichroic mirror, F_{EM}: Emission filter, TL: Tube lens. Pump 1-3: pressure-based pumps.

around (0.76 ± 0.12) ns, and the fluorescence lifetime of dead cells appears around (1.06 ± 0.15) ns in-flow.

At 0.84 ns, a clear threshold can be drawn that allows sorting under the indicated conditions. Using 0.84 ns as the threshold for a hypothetical sorting experiment would result in an accuracy of 96% for properly sorted live cells and 88% for properly sorted dead cells. The lower fluorescence lifetimes in the FLIM scans could be due to the temperature differences caused by the measurement[25], as the exposure times are very different (up to minutes in the FLIM scans and up to µs in the flow).

While Fluorescence lifetime is usually independent of the applied laserpower[25], photosystems have a special position. So there are some reports in the literature that describe the fluorescence lifetime's dependence on exposure intensity.[41] This is reasoned in the complex connection, of photosysnthesis as a complex quenching mechanism[51–54]. Since the scans were carried out using a different laser power (67 µW instead of 220 µW in-flow) differences in exposure time, we suggest that chosen experimental parameters are decisive for this shift. However, for in-flow measurement and sorting, the lifetime difference between living and dead cells was distinctive, allowing us to proceed with sorting experiments.

Sorting experiments

The actuation of the droplets was realized via two pairs of electrodes that shifted the trajectory of the droplets using

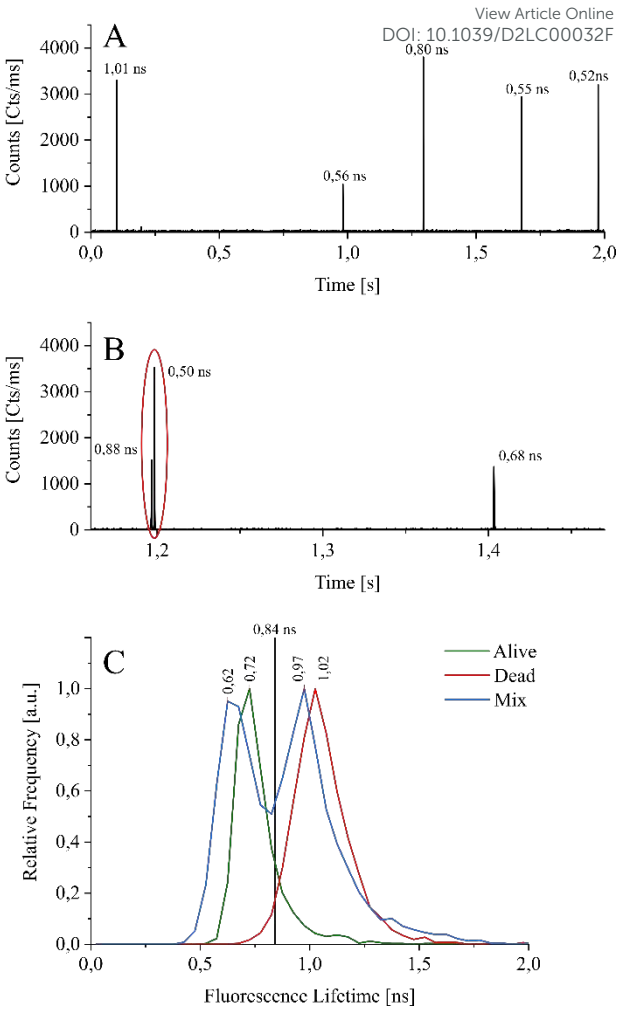

Figure 6: A and B) Intensity feeds of the fluorescence lifetime setup. The calculated fluorescence lifetime of every peak is indicated. B) Intensity feed showing two detected cells in one droplet. C) Fluorescence lifetime histogram of living, dead cyanobacteria and a mixture of living and dead cyanobacteria.

dielectrophoretic (DEP) pulses. One electrode pair was used to actuate dead and live cells, respectively. For cell sorting, we decided to use three flow channels. The upper and the lower channel are for dead and living cells. The middle one is for droplets containing either no cell or for droplets with insufficient signal intensity. We used a commercial desktop computer for the calculation of the fluorescence lifetimes. The calculation time for each calculated fluorescence lifetime was a nearly random number mostly between 5 and 100 ms. Our software EasyFlux was designed to actuate the DEP electrodes after a set and constant time that had to be higher than the maximum calculation time. Dependent on the calculated fluorescence lifetime and the pre-set sorting threshold, the electrode pairs for sorting were actuated.

Since the droplets were moving fast, we detected them 5 mm apart from the sorting area (Figure 4D). The droplets' time between getting detected and arriving in the sorting area was measured using a high-speed camera and the distance markers as displayed in Figure 4C. High throughput sorting is made possible by the high-speed camera, which ensures

View Article Online
DOI: 10.1039/D2LC00035E

synchronization of triggering and detection even at high droplet frequencies. The increased linear droplet velocities also enhanced the system's overall stability, which allows sorting over a time of several hours at high sorting accuracy. Crucial input parameters are droplet frequency and the degree of encapsulation of individual cells, which can be described by the Poisson distribution.[44] The combination of these input parameters affects the detection probability, accuracy, and overall throughput from a cell sorting perspective. We aimed for a frequency of 0.3 cells per droplet or less to ensure approximately single cell encapsulation. The sorting experiments were performed at droplet frequencies between 60 and 100 Hz. A high-speed video of the sorting is in the supplemental materials. Overall, we achieved a throughput of 2.4 to 12.8 cells per second, sorted as live or dead. A detailed discussion of the parameters chosen for sorting is given in the SI.

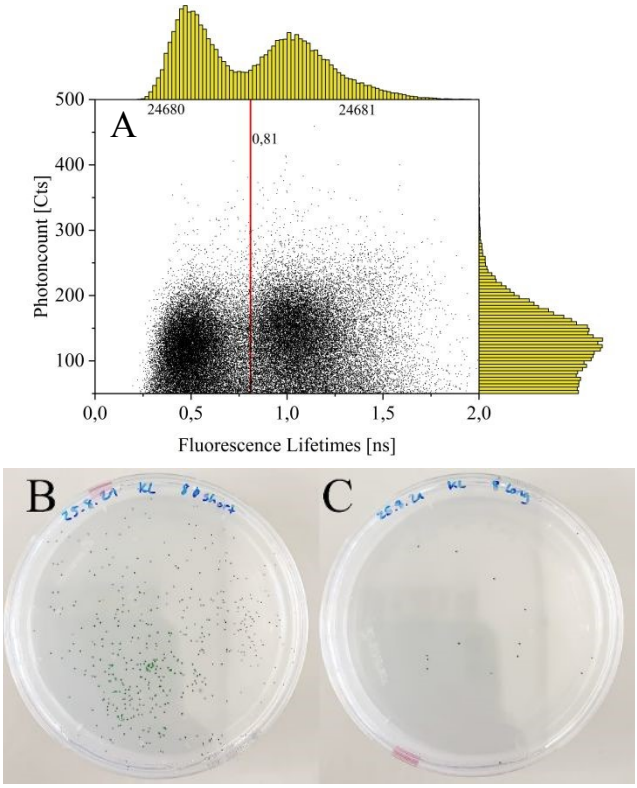

Figure 7: A) Marginal histogram of every recorded cell during the sorting experiments. The Fluorescence Lifetime and the number of photons considered for the calculation of the fluorescence lifetimes are indicated. On the upper edge, a histogram shows how often every fluorescence lifetime appeared. On the left edge, a histogram indicates how often every photon count appeared. The red line indicates the threshold for sorting at 0.81 ns. Also, the number of cells sorted on each side of the threshold is indicated. B) Agar-agar plate with cultured cells with fluorescence lifetime below the threshold. C) Agar-agar plate with cultured cells with fluorescence lifetime above the threshold.

The recorded data are shown in Figure 7A. In the plot, every black dot marks a detected cell. The fluorescence lifetime is given on the abscissa, and the photons considered for calculating the fluorescence lifetime are marked on the ordinate. The fluorescence lifetime histogram is shown on the upper part of the diagram, and the intensity histogram is shown on the right side of the histogram. The red line indicates the sorting lifetime threshold of the sorting experiments. Also, the number of calculated lifetimes below or above the threshold is marked in the diagram. It is apparent that two clouds of data points can be clearly distinguished. The dots in the area with lower lifetimes left from the threshold represent the cells that are considered alive. The dots in the area with higher lifetimes right from the threshold represent the cells considered dead. It is noticeable that the number of photons considered seems to be slightly increased on average in the dead cells due to their increased fluorescence yield. We decided to plate the sorted fractions on yBG11 agar plates to verify that the cells were spectroscopically assigned and sorted as alive actually were. The Agar-plates were incubated until cell colonies were visible. For the displayed sorting experiment, the agar-agar plate in Figure 7B indicates the culture of the sorted living cells, which shows 353 colonies. The agar-agar plate in Figure 7C shows only 13 colonies. Using the calculation described in the Materials and methods gives sorting accuracy between 86 % and 97 %.

We performed a series of independent sorting experiments, of which the histograms and photographs of the agar-agar plates are shown in the supplementary information. The number of sorted cells considered live and dead, the sorting threshold, the volume of the cell suspension, its plated fraction, the percentage of grown cells, and the resulting accuracy are displayed in Table 1 (SI). In our sorting experiments, we achieved accuracies of up to 97%. One possible error source is the level of single-cell encapsulation. If a droplet contains more than one cell, the droplet is sorted based on the fluorescence lifetime of one cell, while the other cells are undefined and might be sorted wrong. Another error source is the overlap in the histograms of the fluorescence lifetimes of living and dead cells, as visible in Figure 6C. When calculating fluorescence lifetimes with low photon counts, the calculated fluorescence lifetime tends to have a higher deviation in FL, which could also cause the false sorting of detected cells. Another error source is the laser's potential phototoxicity that might kill some living cells during excitation.

Influence of stressors on cyanobacteria lifetime

To demonstrate the feasibility of our developed approach, we investigated the sorting system's applicability for studying the physiological stress responses of *Synechocystis* sp. PCC6803. In nature, many strains of cyanobacteria exist. With our system, we attempted to screen the fluorescence lifetime of *Synechocystis* sp. PCC6803 wild-type and the respective NDH-1-deficient M55 mutant strain. The mutant strains deficiency in NDH-1 causes increased sensitivity of the cells photosystem 1 (PSI) to environmental stress, resulting in altered photosynthesis physiology compared to the wild-type strain. Furthermore, we investigated the effect of the antibiotic kanamycin (Km) and increased light and CO_2 exposure on the cells. All influence factors were screened in comparison to untreated *Synechocystis* sp. PCC6803 wild-type samples. The plots of the influencing factors tested are shown in Figure 8. In comparison to sorting experiments, the inclusion of a highspeed camera was not necessary. Since no light from a secondary light

View Article Online
DOI: 10.1039/D2LC00030E

source (see Figure 5) had to be filtered out, we used a 420 nm long-pass filter instead of a 510 nm long-pass filter allowing us to collect a higher fraction of the fluorescence of the cells, but also more noise. Regarding fluorescence lifetimes of *Synechocystis* sp. PCC6803 wild-type cyanobacteria, this resulted in an overall higher fluorescence lifetime of 0.85 ± 0.09 instead of 0.76 ± 0.12. The M55 mutant exhibits a fluorescence lifetime of (0.74 ± 0.07) ns, 100 fs lower than the wild-type with a fluorescence lifetime of (0.85 ± 0.09) ns, which could be reasoned in the changed photosynthesis functioning. In comparison to *Synechocystis* sp. PCC6803 wild-type, the M55 mutant carries a defective NAD(P)H-dehydrogenase.[55] Wild-type and M55-mutant show considerable overlap in their fluorescence lifetime distribution, as discussed in the SI. This overlap would complicate the fluorescence lifetime-based sorting of both strains. Besides that, the result indicates that the developed system can screen for heterogeneity and alterations of the photosynthesis machinery in mutant strains of cyanobacteria.

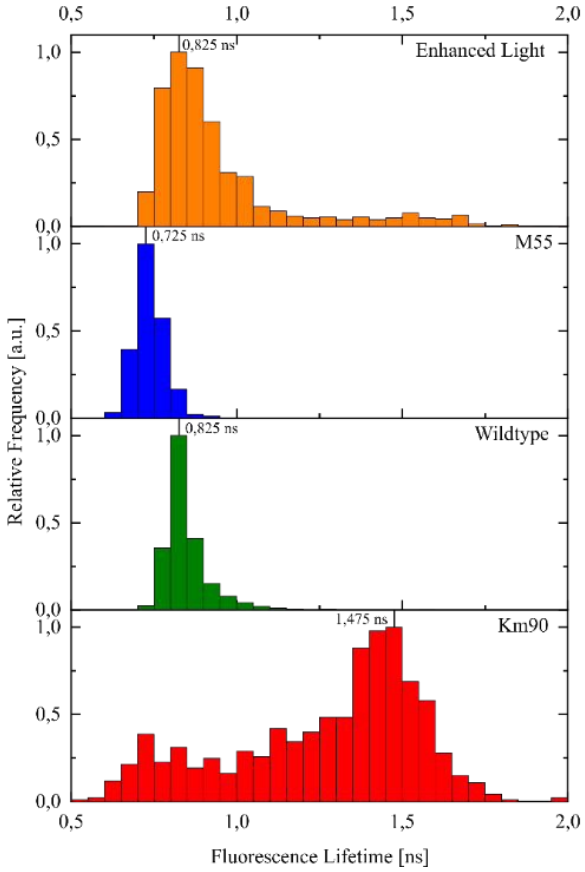

Figure 8: Influence of different conditions and stressors on the fluorescence Lifetime of cyanobacteria. Green: Wildtype Cyanobacteria for comparison. Blue: M55 mutant of cyanobacteria. Orange: the influence of enhanced Light exposure and enhanced CO_2 levels. Red: the influence of Km 90 toxin on wild-type cyanobacteria.

Another important stress factor for cyanobacteria is enhanced light exposure. However, by increasing the CO_2 supply to the cell, the effect of light stress can be reduced due to the increased availability of carbon as a sink for electrons from photosynthesis. The sample of *Synechocystis* sp. PCC6803 treated with these conditions showed that the distribution of fluorescence lifetimes was broadened compared to normally cultured wild-type *Synechocystis* sp. PCC6803, while the peak position in the histogram stayed at the same place of 0.825 ns. These results indicate a differential response within the culture to light stress conditions. However, they can barely be used for sorting. The light-stressed *Synechocystis* sp. PCC6803 sample showed a significantly higher abundance of cells with enhanced fluorescence lifetimes above 1.0 ns, which is a potential indicator for cell stress. This indicates that with the help of the established system, we can investigate and quantify the influence of light and CO_2 levels, which can be used to optimize biotechnological applications and analyze potential environmental stressors without using external dyes stains.

Toxins can also affect the fluorescence lifetime of cyanobacteria, as we already showed by fixating them with PFA. Next to PFA, the response of photosynthesis performance and cellular viability to extracellular toxins is of broad interest. We chose Km90 conditions (kanamycin at a final concentration of 90 µg mL^{-1}) as a proxy for the effect of other toxins on the physiology of *Synechocystis* sp. PCC6803. The influence of Km90 on a bulk solution of wild-type c *Synechocystis* sp. PCC6803 is displayed in Figure 8. The histogram shows a maximum at 1.475 ns. However, a significant number of cells appear in a fluorescence lifetime below 1.0 ns, which is a potential indicator for their fluorescence activity, indicating that they might have survived being treated with Km90. These results prove that our system is useful for investigating the differential stress response of cyanobacteria to toxins with single-cell resolution.

Conclusions

In this proof of concept study, the autofluorescence lifetimes of the photosynthetic machinery in *Synechocystis* sp. PCC6803 was harnessed to sort single cyanobacterial cells in droplets based on their physiological status. For this purpose, the fluorescence and fluorescence lifetime properties of *Synechocystis* sp. PCC6803 were studied. Furthermore, the FLADS platform established in our previous studies was optimized for detecting and sorting cells. Combining the fluorescence lifetime technique with droplet microfluidics allowed us to establish a non-lethal technique for label-free in-flow single-cell analysis and sorting. With the sorting of living and dead *Synechocystis* sp. PCC6803, we proved the usability of fluorescence lifetime-based droplet sorting. Furthermore, we showed its usability in studying the behaviour of *Synechocystis* sp. PCC6803 regarding different genetic backgrounds, environmental factors, and toxins aiming directly at the functionality of their photosynthetic machinery. Going forward, we established FLADS as a powerful tool for studying phototrophic microbes at a single-cell level while enabling the recovery of specific photosynthesis phenotypes for further systematic experiments such as examining their heterogeneity and secretion. Fluorescence lifetime offers an additional stainless sorting criterion complementing absorption or fluorescence alone. Incorporating fluorescence lifetime has the potential to connect

studying the secretion in dependency of the functionality of the photosynthesis apparatus.
Reducing channel dimensions or incorporating particle focusing techniques [56,57] as ultrasonic waves[58,59] could improve the comparatively low cell detection probability of 30%.

Acknowledgments

We thank Kristin Lindsteadt and Anish Das for their technical support.

Conflict of Interest

The authors have no conflicts of interest to declare. All co-authors have seen and agree with the manuscript's contents, and there is no financial interest to report. We certify that the submission is original work and is not under review at any other publication.

References

1 L. Shang, Y. Cheng and Y. Zhao, Emerging Droplet Microfluidics, *Chem. Rev.*, 2017, **117**, 7964–8040.
2 S.-Y. Teh, R. Lin, L.-H. Hung and A. P. Lee, Droplet microfluidics, *Lab Chip*, 2008, **8**, 198–220.
3 G. M. Whitesides, The origins and the future of microfluidics, *nature*, 2006, **442**, 368–373.
4 T. S. Kaminski and P. Garstecki, Controlled droplet microfluidic systems for multistep chemical and biological assays, *Chem. Soc. Rev.*, 2017, **46**, 6210–6226.
5 I. Shestopalov, J. D. Tice and R. F. Ismagilov, Multi-step synthesis of nanoparticles performed on millisecond time scale in a microfluidic droplet-based system, *Lab Chip*, 2004, **4**, 316–321.
6 Y. Wang, Z. Chen, F. Bian, L. Shang, K. Zhu and Y. Zhao, Advances of droplet-based microfluidics in drug discovery, *Expert Opinion on Drug Discovery*, 2020, **15**, 969–979.
7 N. Shembekar, C. Chaipan, R. Utharala and C. A. Merten, Droplet-based microfluidics in drug discovery, transcriptomics and high-throughput molecular genetics, *Lab Chip*, 2016, **16**, 1314–1331.
8 L. Armbrecht and P. S. Dittrich, Recent Advances in the Analysis of Single Cells, *Anal. Chem.*, 2017, **89**, 2–21.
9 D. Hümmer, F. Kurth, N. Naredi-Rainer and P. S. Dittrich, Single cells in confined volumes: microchambers and microdroplets, *Lab Chip*, 2016, **16**, 447–458.
10 H. N. Joensson and H. Andersson Svahn, Droplet microfluidics--a tool for single-cell analysis, *Angewandte Chemie (International ed. in English)*, 2012, **51**, 12176–12192.
11 K. Matuła, F. Rivello and W. T. S. Huck, Single-Cell Analysis Using Droplet Microfluidics, *Adv. Biosys.*, 2020, **4**, e1900188.
12 L. Mazutis, J. Gilbert, W. L. Ung, D. A. Weitz, A. D. Griffiths and J. A. Heyman, Single-cell analysis and sorting using droplet-based microfluidics, *Nat Protoc*, 2013, **8**, 870–891.
13 M. Girault, H. Kim, H. Arakawa, K. Matsuura, M. Odaka, A. Hattori, H. Terazono and K. Yasuda, An on-chip imaging droplet-sorting system: a real-time shape recognition method to screen target cells in droplets with single cell resolution, *Sci Rep*, 2017, **7**, 40072.
14 J.-C. Baret, O. J. Miller, V. Taly, M. Ryckelynck, A. El-Harrak, L. Frenz, C. Rick, M. L. Samuels, J. B. Hutchison, J. J. Agresti, D. R. Link, D. A. Weitz and A. D. Griffiths, Fluorescence-activated droplet sorting (FADS): efficient microfluidic cell sorting based on enzymatic activity, *Lab Chip*, 2009, **9**, 1850–1858.
15 Y. Zhu and Q. Fang, Analytical detection techniques for droplet microfluidics--a review, *Analytica Chimica Acta*, 2013, **787**, 24–35.
16 S. Mashaghi, A. Abbaspourrad, D. A. Weitz and A. M. van Oijen, Droplet microfluidics: A tool for biology, chemistry and nanotechnology, *Trends Anal. Chem.*, 2016, **82**, 118–125.
17 D. Vallejo, A. Nikoomanzar, B. M. Paegel and J. C. Chaput, Fluorescence-Activated Droplet Sorting for Single-Cell Directed Evolution, *ACS Synth. Biol.*, 2019, **8**, 1430–1440.
18 M. Herbig, K. Tessmer, M. Nötzel, A. A. Nawaz, T. Santos-Ferreira, O. Borsch, S. J. Gasparini, J. Guck and M. Ader, *Label-free imaging flow cytometry: analysis and sorting of enzymatically dissociated tissues*, 2021.
19 F. Gielen, R. Hours, S. Emond, M. Fischlechner, U. Schell and F. Hollfelder, Ultrahigh-throughput-directed enzyme evolution by absorbance-activated droplet sorting (AADS), *Proc Natl Acad Sci USA*, 2016, **113**, E7383-E7389.
20 X. Wang, L. Ren, Y. Su, Y. Ji, Y. Liu, C. Li, X. Li, Y. Zhang, W. Wang, Q. Hu, D. Han, J. Xu and B. Ma, Raman-Activated Droplet Sorting (RADS) for Label-Free High-Throughput Screening of Microalgal Single-Cells, *Anal. Chem.*, 2017, **89**, 12569–12577.
21 D. A. Holland-Moritz, M. K. Wismer, B. F. Mann, I. Farasat, P. Devine, E. D. Guetschow, I. Mangion, C. J. Welch, J. C. Moore, S. Sun and R. T. Kennedy, Mass Activated Droplet Sorting (MADS) Enables High-Throughput Screening of Enzymatic Reactions at Nanoliter Scale, *Angewandte Chemie (International ed. in English)*, 2020, **59**, 4470–4477.
22 B. Y. Yu, C. Elbuken, C. Shen, J. P. Huissoon and C. L. Ren, An integrated microfluidic device for the sorting of yeast cells using image processing, *Sci Rep*, 2018, **8**, 3550.
23 E. Zang, S. Brandes, M. Tovar, K. Martin, F. Mech, P. Horbert, T. Henkel, M. T. Figge and M. Roth, Real-time image processing for label-free enrichment of Actinobacteria cultivated in picolitre droplets, *Lab Chip*, 2013, **13**, 3707–3713.
24 F. Jamme, S. Kascakova, S. Villette, F. Allouche, S. Pallu, V. Rouam and M. Réfrégiers, Deep UV autofluorescence microscopy for cell biology and tissue histology, *Biol. Cell*, 2013, **105**, 277–288.
25 M. Y. Berezin and S. Achilefu, Fluorescence lifetime measurements and biological imaging, *Chem. Rev.*, 2010, **110**, 2641–2684.
26 D. Campbell, V. Hurry, A. K. Clarke, P. Gustafsson and G. Oquist, Chlorophyll fluorescence analysis of cyanobacterial

photosynthesis and acclimation, *Microbiol Mol Biol Rev*, 1998, **62**, 667–683.

27 J. P. Houston, M. A. Naivar and J. P. Freyer, Digital analysis and sorting of fluorescence lifetime by flow cytometry, *Cytom. A*, 2010, **77**, 861–872.

28 J. Nedbal, V. Visitkul, E. Ortiz-Zapater, G. Weitsman, P. Chana, D. R. Matthews, T. Ng and S. M. Ameer-Beg, Time-domain microfluidic fluorescence lifetime flow cytometry for high-throughput Förster resonance energy transfer screening, *Cytom. A*, 2015, **87**, 104–118.

29 R. Cao, V. Pankayatselvan and J. P. Houston, Cytometric sorting based on the fluorescence lifetime of spectrally overlapping signals, *Opt. Express*, 2013, **21**, 14816–14831.

30 B. P. Yakimov, M. A. Gogoleva, A. N. Semenov, S. A. Rodionov, M. V. Novoselova, A. V. Gayer, A. V. Kovalev, A. I. Bernakevich, V. V. Fadeev, A. G. Armaganov, V. P. Drachev, D. A. Gorin, M. E. Darvin, V. I. Shcheslavskiy, G. S. Budylin, A. V. Priezzhev and E. A. Shirshin, Label-free characterization of white blood cells using fluorescence lifetime imaging and flow-cytometry: molecular heterogeneity and erythrophagocytosis Invited, *Biomed. Opt. Express*, 2019, **10**, 4220–4236.

31 S. Hasan, D. Geissler, K. Wink, A. Hagen, J. J. Heiland and D. Belder, Fluorescence lifetime-activated droplet sorting in microfluidic chip systems, *Lab Chip*, 2019, **19**, 403–409.

32 S. Hasan, M. E. Blaha, S. K. Piendl, A. Das, D. Geissler and D. Belder, Two-photon fluorescence lifetime for label-free microfluidic droplet sorting, *Analytical and bioanalytical chemistry*, 2021. DOI: 10.1007/s00216-021-03745-2.

33 I. Chorus and J. Bartram, *Toxic cyanobacteria in water. A guide to their public health consequences, monitoring, and management*, E & FN Spon, London, New York, 1999.

34 J. C. Nabout, B. da Silva Rocha, F. M. Carneiro and C. L. Sant'Anna, How many species of Cyanobacteria are there? Using a discovery curve to predict the species number, *Biodivers. Conserv.*, 2013, **22**, 2907–2918.

35 S. L. Percival and D. W. Williams, in *Microbiology of waterborne diseases*, ed. S. L. Percival, Academic Press; Elsevier, London, Amsterdam, Heidelberg, 2nd edn., 2014, pp. 79–88.

36 Z. Zahra, H. Da Choo, H. Lee and A. Parveen, Cyanobacteria: Review of Current Potentials and Applications, *Environments*, 2020, **7**, 13.

37 F. Branco dos Santos, W. Du and K. J. Hellingwerf, Synechocystis: Not Just a Plug-Bug for CO2, but a Green E. coli, *Front. Bioeng. Biotechnol.*, 2014, **2**, 36.

38 Y. Yu, Le You, D. Liu, W. Hollinshead, Y. J. Tang and F. Zhang, Development of Synechocystis sp. PCC 6803 as a phototrophic cell factory, *Marine Drugs*, 2013, **11**, 2894–2916.

39 Edith Bittersmann and Wim Vermaas, Fluorescence lifetime studies of cyanobacterial photosystem II mutants, *BBA – Bioenergetics*, 1991, **1098**, 105–116.

40 E. Bittersmann and W. Vermaas, Fluorescence lifetime studies of cyanobacterial photosystem II mutants, *Biochim. Biophys. Acta*, 1991, **1098**, 105–116.

41 S. Nozue, A. Mukuno, Y. Tsuda, T. Shiina, M. Terazima and S. Kumazaki, Characterization of thylakoid membrane in a heterocystous cyanobacterium and green alga with dual-detector fluorescence lifetime imaging microscopy with a systematic change of incident laser power, *Biochim. Biophys. Acta*, 2016, **1857**, 46–59.

42 A. F. Bhatti, R. R. Choubeh, D. Kirilovsky, E. Wientjes and H. van Amerongen, State transitions in cyanobacteria studied with picosecond fluorescence at room temperature, *Biochimica et biophysica acta. Bioenergetics*, 2020, **1861**, 148255.

43 M. Schirmer, K. Wink, S. Ohla, D. Belder, A. Schmid and C. Dusny, Conversion Efficiencies of a Few Living Microbial Cells Detected at a High Throughput by Droplet-Based ESI-MS, *Anal. Chem.*, 2020, **92**, 10700–10708.

44 D. J. Collins, A. Neild, A. deMello, A.-Q. Liu and Y. Ai, The Poisson distribution and beyond: methods for microfluidic droplet production and single cell encapsulation, *Lab Chip*, 2015, **15**, 3439–3459.

45 S. Shcolnick, Y. Shaked and N. Keren, A role for mrgA, a DPS family protein, in the internal transport of Fe in the cyanobacterium Synechocystis sp. PCC6803, *Biochimica et biophysica acta*, 2007, **1767**, 814–819.

46 J. Zhao, F. Gao, D.-Y. Fan, W. S. Chow and W. Ma, NDH-1 Is Important for Photosystem I Function of Synechocystis sp. Strain PCC 6803 under Environmental Stress Conditions, *Front. Plant Sci.*, 2017, **8**, 2183.

47 J. Linnanto and J. Korppi-Tommola, Quantum chemical simulation of excited states of chlorophylls, bacteriochlorophylls and their complexes, *Phys. Chem. Chem. Phys.*, 2006, **8**, 663–687.

48 H. K. Lichtenthaler, G. Langsdorf, S. Lenk and C. Buschmann, Chlorophyll fluorescence imaging of photosynthetic activity with the flash-lamp fluorescence imaging system, *Photosynt.*, 2005, **43**, 355–369.

49 H. J. Keuper and K. Sauer, Effect of photosystem II reaction center closure on nanosecond fluorescence relaxation kinetics, *Photosynth Res*, 1989, **20**, 85–103.

50 J. Cao and Govindjee, Chlorophyll a fluorescence transient as an indicator of active and inactive photosystem II in thylakoid membranes, *Biochimica et Biophysica Acta (BBA) - Bioenergetics*, 1990, **1015**, 180–188.

51 T. M. Nordlund and W. H. Knox, Lifetime of fluorescence from light-harvesting chlorophyll a/b proteins. Excitation intensity dependence, *Biophysical Journal*, 1981, **36**, 193–201.

52 R. C. Dunn, G. R. Holtom, L. Mets and X. S. Xie, Near-Field Fluorescence Imaging and Fluorescence Lifetime Measurement of Light Harvesting Complexes in Intact Photosynthetic Membranes, *J. Phys. Chem.*, 1994, **98**, 3094–3098.

53 A. J. Campillo, S. L. Shapiro, V. H. Kollman, K. R. Winn and R. C. Hyer, Picosecond exciton annihilation in photosynthetic systems, *Biophysical Journal*, 1976, **16**, 93–97.

54 A. J. Campillo, V. H. Kollman and S. L. Shapiro, Intensity Dependence of the Fluorescence Lifetime of in vivo Chlorophyll

View Article Online
DOI: 10.1039/D2LC00032F

Excited by a Picosecond Light Pulse, *Science*, 1976, **193**, 227–229.

55 J. Olive, G. Ajlani, C. Astier, M. Recouvreur and C. Vernotte, Ultrastructure and light adaptation of phycobilisome mutants of Synechocystis PCC 6803, *Biochimica et Biophysica Acta (BBA) - Bioenergetics*, 1997, **1319**, 275–282.

56 X. Xuan, J. Zhu and C. Church, Particle focusing in microfluidic devices, *Microfluid Nanofluid*, 2010, **9**, 1–16.

57 M. Tenje, A. Fornell, M. Ohlin and J. Nilsson, Particle Manipulation Methods in Droplet Microfluidics, *Anal. Chem.*, 2018, **90**, 1434–1443.

58 A. Fornell, F. Garofalo, J. Nilsson, H. Bruus and M. Tenje, Intra-droplet acoustic particle focusing: simulations and experimental observations, *Microfluid Nanofluid*, 2018, **22**. DOI: 10.1007/s10404-018-2094-9.

59 A. Fornell, H. Pohlit, Q. Shi and M. Tenje, Acoustic focusing of beads and cells in hydrogel droplets, *Sci Rep*, 2021, **11**, 7479.